Trading coherence and entropy by a quantum Maxwell demon

A. V. Lebedev, D. Oehri, G. B. Lesovik, and G. Blatter

Phys. Rev. A **94**, 052133 — Published 28 November 2016

DOI: 10.1103/PhysRevA.94.052133

Trading coherence and entropy by a quantum Maxwell demon

A.V. Lebedev,[1] D. Oehri,[1] G.B. Lesovik,[2,3,1] and G. Blatter[1]

[1] *Theoretische Physik, Wolfgang-Pauli-Strasse 27, ETH Zurich, CH-8093 Zürich, Switzerland*
[2] *L.D. Landau Institute for Theoretical Physics RAS, Akad. Semenova av. 1-A, Chernogolovka, 142432, Moscow Region, Russia*
[3] *Moscow Institute of Physics and Technology, Institutskii per. 9, 141700 Dolgoprudny, Moscow District, Russia*

(Dated: November 3, 2016)

The Second Law of Thermodynamics states that the entropy of a closed system is non-decreasing. Discussing the Second Law in the quantum world poses new challenges and provides new opportunities, involving fundamental quantum-information-theoretic questions and novel quantum-engineered devices. In quantum mechanics, systems with an evolution described by a so-called unital quantum channel evolve with a non-decreasing entropy. Here, we seek the opposite, a system described by a non-unital and, furthermore, energy-conserving channel that describes a system whose entropy decreases with time. We propose a setup involving a mesoscopic four-lead scatterer augmented by a micro-environment in the form of a spin that realizes this goal. Within this non-unital and energy-conserving quantum channel, the micro-environment acts with two non-commuting operations on the system in an autonomous way. We find, that the process corresponds to a partial exchange or swap between the system and environment quantum states, with the system's entropy decreasing if the environment's state is more pure. This entropy-decreasing process is naturally expressed through the action of a quantum Maxwell demon and we propose a quantum-thermodynamic engine with four qubits that extracts work from a single heat reservoir when provided with a reservoir of pure qubits. The special feature of this engine, which derives from the energy-conservation in the non-unital quantum channel, is its separation into two cycles, a working cycle and an entropy cycle, allowing to run this engine with no local waste heat.

PACS numbers:

I. INTRODUCTION

The conversion of heat into useful energy or work is at the very heart of the Second Law of Thermodynamics[1], rendering the design and functionality of thermodynamic engines a recurrent topic. Although dealing with such seemingly prosaic issues as the efficiency of a machine[2], the Second Law implies drastic consequences, telling which processes are allowed to occur in nature, an example being the requirement of non-decreasing entropy in an isolated system. New opportunities and challenges appear when taking the Second Law of Thermodynamics into the quantum regime. In early work on open quantum systems the Second Law could be derived within a quantum master equation approach assuming a weak coupling between the system and thermal reservoirs[3,4]. More recently, other types of reservoirs and couplings have been included and the topic has likewise caught the interest of the quantum-information and quantum-engineering communities, with recent work addressing both fundamental[5–9] and practical[10–15] issues. Equally pertinent to the topic is Maxwell's demon[16,17] and its taming by Landauer's principle[18–20], adding the concept of information to the discussion[22,23]. In this paper, we invoke a quantum demon that makes use of quantum purity to decrease the entropy and increase the coherence of an energetically isolated system. Starting from statement that the entropy is non-decreasing in a unital quantum channel[26], we search for the characteristics of a non-unital quantum channel that allows for a maximal decrease of entropy in an (energy-)isolated system. We find that such a non-unital quantum channel involves a quantum demon that is swapping external pure quantum states against mixed system states, see Fig. 1. We present three specific examples for such demons, two mesoscopic systems using a spin or a double quantum-dot as part of the demon that imprints a coherent state on an incoherent electron (and thus decreases the electron's entropy), and a four-qubit system constituting a quantum thermodynamic engine with separated energy and entropy cycles.

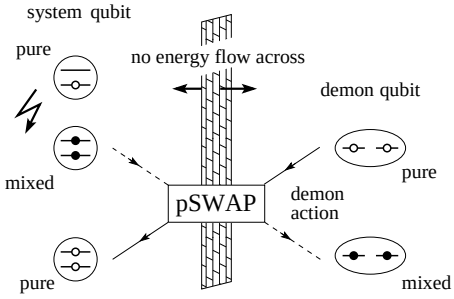

FIG. 1: Purification of an energetically isolated system with the help of a quantum demon. The system qubit on the left undergoes a transition (arrow) to a mixed state (full circles), e.g., by decoherence or through thermal excitation. The demon makes use of a pure demon qubit (right, open circles) and swaps its state with the system qubit, thereby transferring entropy or coherence but no energy.

A fully isolated quantum system evolves unitarily and

hence its entropy remains constant, rendering the Second Law a triviality. A non-trivial setting is defined by an open quantum system[21]. Here, we have in mind a system that is energetically isolated (and keeps a fixed particle number) but can decrease its entropy through entanglement with its environment. This entanglement between the system and the environment can be induced with the help of a phase-like interaction. Importantly, such a phase-exchange mechanism does not require an exchange of energy, thus modifying the concept of classical isolation when dealing with an open quantum system. Indeed, it is well known that typical quantum systems become more rapidly entangled through a phase-exchange process than through a relaxation process, as prominently expressed by the scale separation of the corresponding relaxation times for phase (T_2) and energy (T_1) in quantum engineered systems. Extensions of the Second Law accounting for the presence of classical (as opposed to quantum) correlations between the system and an information reservoir has recently been discussed in Refs. [22,23].

In a typical situation, the quantum system interacts with a large environment that induces dephasing, eliminating the off-diagonal components of the system's density matrix and increasing its entropy. However, if the environment is a small and controllable quantum system, we will show below that one can tune the interaction between the system and the environment in such a way as to decrease the system's entropy. Furthermore, using a phase exchange mechanism without energy exchange with the environment, such a decrease in entropy leads to an apparent contradiction to the traditional classical formulation of the Second Law. In our discussion below, this entropy decrease will be achieved by a quantum demon using a SWAP operation in order to exchange purity (or coherence) between the micro environment and the quantum system. Including the micro environment in the entropy balance of the grand system reestablishes the Second Law (via Landauer's principle) in a proper way.

The standard description of the above situation (an open quantum system initially disentangled from its environment) is given by a *quantum channel* Φ. In its mathematical formulation, this is a completely positive, trace-preserving map that transforms the initial density matrix $\hat{\rho}_0$ of the quantum system to a new density matrix $\hat{\rho} = \Phi(\hat{\rho}_0)$. In our physical context, $\Phi = \Phi_t$ describes the evolution of the system's density matrix, $\hat{\rho}_t = \mathrm{Tr}_{\mathrm{env}}[\hat{U}(t,t_0)\hat{\rho}_0\hat{U}^\dagger(t,t_0)] \equiv \Phi_t(\hat{\rho}_0)$, under the inclusion of the environment ($\hat{U}(t,t_0)$ denotes the evolution of the grand system). The entropy of such an open quantum system is not conserved, $S[\Phi(\hat{\rho}_0)] \neq S(\hat{\rho}_0)$, and actually can both increase and decrease. Exploiting the monotonicity of the relative entropy[24] in a quantum channel[25], one can show[26] that the change in the entropy itself is bounded from below, $S[\Phi(\hat{\rho}_0)] - S(\hat{\rho}_0) \geq -\mathrm{Tr}\big\{[\Phi(\hat{\rho}_0)]\,\ln\Phi(\mathbb{1}))\big\}$. It follows that a special subclass of quantum channels which preserve the identity operator, $\Phi(\mathbb{1}) = \mathbb{1}$, has a non-negative entropy gain, $\ln(\mathbb{1}) = 0$ and hence $S[\Phi(\hat{\rho}_0)] - S(\hat{\rho}_0) \geq 0$.

A quantum system whose evolution can be described by a an identity-preserving quantum channel evolves with a non-decreasing entropy, $S[\Phi(\hat{\rho}_0)] \geq S(\hat{\rho}_0)$; such a quantum channel is called unital. It turns out that for finite dimensional quantum systems, unitality is not only a sufficient but also a necessary condition for a non-negative entropy gain. Indeed, if a N-dimensional quantum system evolves with non-decreasing entropy for any initial state $\hat{\rho}_0$, then it does so also for the completely chaotic state $\hat{\rho}_c = \mathbb{1}/N$ and therefore $S[\Phi(\hat{\rho}_c)] \geq S(\hat{\rho}_c)$. Since the chaotic state $\hat{\rho}_c$ has maximal possible entropy $k_{\mathrm{B}}\ln(N)$ one has $S[\Phi(\hat{\rho}_c)] = k_{\mathrm{B}}\ln(N)$ and hence $\Phi(\hat{\rho}_c) = \mathbb{1}/N$, that proves the unitality of Φ. Note, that unitality does not imply energy conservation of a quantum channel. Indeed, consider a quantum channel $\Phi(\hat{\rho}) = \hat{P}\big(\mathrm{diag}(\hat{\rho})\big)$ which eliminates all off-diagonal elements of the density matrix and imposes an arbitrary permutation $\hat{P}$ of its diagonal elements. This quantum channel is unital, however, the permutation of the diagonal elements in an energy representation does not conserve the total energy of the quantum system.

These considerations tell us that in order to find a finite-dimensional quantum system whose entropy decreases under its evolution, we have to search for a non-unital quantum channel and a suitable initial state. A non-unital channel can be trivially realized if the condition of energy isolation is abandoned. E.g., the long time evolution of a quantum system weakly interacting with a thermal environment in non-unital. Indeed, at large times $t \gg T_1$, the quantum system equilibrizes with the environment, $\Phi(\mathbb{1}) \to \hat{\rho}_{\mathrm{th}} \neq \mathbb{1}/N$, and the system's change of entropy is defined by the net heat flow between the system and the environment, $\Delta S = \Delta Q/T$. In contrast, here we are interested in a less trivial situation where the system is energetically isolated and hence we have to search for an energy-preserving non-unital channel.

The existence of energy-preserving non-unital quantum channels that reduce the entropy has been pointed out in Ref. [27]: scattering an electron in a three-terminal mesoscopic conductor suitably interacting with a spin, reduces the entropy of the outgoing state with respect to the incoming one. Below, we investigate the functionality of such a quantum channel in more detail and find conditions and specific examples that lead to a maximal decrease of entropy. We will present two mesoscopic scattering setups that define such energy-preserving non-unital quantum channels with initial states that evolve with maximal decreasing entropy. In both examples, we consider a four-lead reflectionless beam splitter and a general incoming electronic state $\hat{\rho}_{\mathrm{in}}$ that is scattered by the symmetric splitter. The system is augmented by an energy-degenerate qubit acting as the microscopic environment. The scattering electron interacts with the qubit in such a way as to define a non-unital quantum channel for the electron that decreases the entropy of

its outgoing state $\hat{\rho}_{\rm out}$ with respect to the incoming one, $S(\hat{\rho}_{\rm out}) \leq S(\hat{\rho}_{\rm in})$, without exchange of energy between the electron and the energy-degenerate qubit. In the first example, the qubit is a suitably prepared spin that interacts with the electron propagating in two of the four leads in the beam splitter. The leads and the position of the spin are arranged such that the electron's propagation through the incoming and outgoing channels generates two spin rotations that do not commute, see Eq. (4) below—the non-commutativity of these two operations, as derived from the non-unitality condition, is a central feature of this setup. In the second example, we replace the spin by a double-quantum-dot that is more easily manipulated in a realistic system. Here, the quantum dot exerts the identical operation on the electron, once in the incoming and a second time in the outgoing lead, however, suitably rotating the double-dot's state in between the two interaction events renders the two operations on the electron effectively non-commuting. Within the mesoscopic transport setting, the reduced entropy in the outgoing lead corresponds to an increase in coherence of the outgoing electron state, where the attained coherence is provided by the demon. The concept may be useful in locally generating a coherent state of a flying qubit using the purity of a (usually more stable) stationary qubit. In order to test the functionality of such a device, we propose to analyze this imposed coherence in a Mach-Zehnder setup.

Analyzing the functionality of these devices in terms of a quantum algorithm, we find that the various steps in the protocol exchange the quantum states of the system and the demon. Rather than a standard SWAP[10,12,13], our considerations lead to a partial SWAP operation (pSWAP) that exchanges states in one sector of the Hilbert space, while producing an incomplete SWAP (a SWAP up to a NOT operation) in the remaining part of the Hilbert space. While a conventional SWAP operation also achieves the functionality of the non-unital quantum channel, its physical implementation is more demanding within the context of the present paper.

The purification of a quantum state in a demon-assisted process can be used in the construction of a quantum thermodynamic engine. The discussion of quantum thermodynamic processes has continuously progressed over the past two decades, see [28] for a recent review. Quantum thermodynamic machines usually involve hot and cold (switchable) thermal reservoirs in combination with a (spectrally tunable) quantum system as an operating medium, see, e.g., Refs. [29–33], often operating in an autonomous manner[34]. Here, we focus on a class of machines that make use of a SWAP operation between states of different purity. This operation is conveniently described within the framework of Maxwell's demon[16,17]. The demon's original[16,17] resource is the ability to distinguish particle motion such as to transfer them unidirectionally between two adjacent volumes, thereby reducing the system's entropy without investing work. The violation of the Second Law in the restricted system then is cured by going over to the larger system including the Maxwell demon. This is the essence of Landauer's principle,[18–20] stating that resetting the demon's memory costs an entropy $k_{\rm B} \ln 2$ per decision. This entropy has to be picked up by a second reservoir, e.g., at a lower temperature T_0, and the putative perpetuum mobile of the second kind transforms into a conventional Carnot machine.

Through swapping the (less pure) system- with a purer demon state, our quantum demon provides the entropy required to have the machine run with only one thermal reservoir, thus replacing Maxwell's classical demon in a quantum thermodynamic engine. This idea has been introduced early on by Lloyd[10] in his construction of a spin-based NMR demon and a proposal for a quantum thermodynamic engine. An atom-based quantum heat engine transforming heat from one reservoir into work has been proposed by Scully[11], with the negentropy[11] consumed in the cycle corresponding to a reservoir of demon qubits within our language. Within a mesoscopic physics context, an engine involving a quantum dot operating as a spin-valve and swapping states through interaction with a sequence of electrons has been proposed recently[15]. Quantum heat engines assisted by similar quantum demons have been described by Quan *et al.*[12], see also Ref. [13], and more recently by Diaz de la Cruz and Martin-Delgado[35]. The SWAP operation is a central element in algorithmic cooling, e.g., of spins in NMR spectroscopy or for NMR based quantum computation[36–38] as well as in the discussion of the smallness of quantum thermodynamic machines[8].

The SWAP-based quantum heat engines proposed so far involve different characteristics and functionalities. E.g., the engines in Refs. [10,12,13] involve working- and demon qubits with gapped spectra and a SWAP between two thermal states. In such a setup the injected heat is only partly transformed into work. This is due to the energy exchange between working- and demon qubits in the SWAP operation, always reducing the work (or incoming heat) by a waste heat. A setup which does not involve an energy exchange with the demon qubit has been proposed in Ref. [35]. This engine makes use of energy-degenerate working- and demon qubits, with the work extracted in a polarization/depolarization process, which requires a slow (adjabatic) process. The ratchet-type engine that charges a capacitor as described in Ref. [15] also does not exchange energy during the SWAP operation; its main difference to our engine is the deterministic production of work in every cycle that is available in our setup, while the ratchet's operation is statistical.

In our version of a demon-assisted thermodynamic engine, we make use of a partial SWAP (pSWAP) operation exchanging the pure state of an energy-degenerate demon qubit (the dit) with the (non-degenerate) working qubit's (the wit's) thermally excited state in an autonomous process. The exchange of quantum states in the pSWAP operation transforms the wit's thermal energy into the directed energy of a pure excited wit state. The wit's

energy then can be extracted and used with the help of suitable quantum manipulations, while the wit's entropy is carried away by the dit after the pSWAP. While the pSWAP exchanges the entropies (or purities) of the wit and dit, the wit's and dit's energies are separately conserved. The separation into distinct energy and entropy cycles with no energy transfer in between then is the most interesting feature of our quantum-thermodynamic engine. In particular, considering only the energy cycle of the wit, it turns out that the local heat-to-work transfer operates with unit efficiency, i.e., the heat absorbed from the thermal reservoir by the wit can be fully converted into directed work. Furthermore, the entropy cycle where the dit is reprepared for the next round of operation can be run separately, in time or space, from the working cycle of the engine; alternatively, the dits can be provided from a previously prepared reservoir of dit states. On the other hand, combining the outcome of both the energy and entropy cycles, i.e., accounting for the state changes of both the wit and the dit, the Second Law and Landauer's Principle are fully respected and the resulting overall efficiency is smaller than the one of a Carnot machine.

It is instructive to compare our quantum thermodynamic engine with a more traditional setup involving a quantum system that is weakly coupled to two thermal reservoirs, a hot (T_h) and a cold (T_c) one. Making use of Spohn and Lebowitz' growth of the entropy production rate σ (involving the change in entropy $\partial_t S$ and the entropy/heat flow exchanged with the thermal reservoirs) under an Lindbladian channel[3], Alicki[4] has shown that a cyclic operation of such a system performs with an efficiency bounded by that of Carnot's cycle, $\eta \leq \eta_{\rm C} = 1 - T_c/T_h$, thus deriving the validity of the Second Law for this setup. Although involving a 'quantum engine', this setup nevertheless exhibits the usual entropy/heat flows into and out of the machine as familiar from a classical heat engine. In contrast, our quantum thermodynamic engine differs in numerous respects from such a setup. In picking up its heat from the hot thermal reservoir in an isochoric process, Clausius law is not satisfied as the transferred energy is limited by the wit's level separation $\Delta_{\rm w}$, while the maximal entropy acceptable by the wit is $k_{\rm B} \ln 2$. Instead of a cold (memoryless) thermal reservoir, our setup involves a quantum demon which cannot accept any energy and which is strongly coupled to the wit. Furthermore, the unitary evolution that generates the entropy flow from the wit subsystem to the dit subsystem leads to a temporary strong entanglement between the wit and the dit during the SWAP process, a process that is beyond the quantum master equation description used in Ref. 3. As a result the functionality of our engine differs largely from the usual one: instead of generating a waste heat, our cycle makes use of purity. Note that this is different from a classical Maxwell demon where the resource is information[22,23]—in our setup no information is generated that is used in the operation of the machine.

In our demon-assisted heat engine, the $\tilde{\rm p}$SWAP operation generates an entropy flow from the wit subsystem to the dit subsystem which results from a quantum mechanical unitary evolution of the joint wit–dit system, with the additional constraint of no energy exchange between two subsystems.

In the following section II, we introduce an electronic scattering problem which includes the interaction with an auxiliary spin (our first type of demon) and formulate the process in the language of a quantum channel to derive the conditions for an energy-preserving and entropy-decreasing non-unital quantum channel. In section III, we proceed with the discussion of a more practical setup using a quantum double-dot as the demon qubit and proceed to describe the functionality of this non-unital quantum channel in terms of a quantum circuit, see Sec. IV. Section V is devoted to our quantum thermodynamic engine with its special property of separate energy and entropy cycles. In section VI, we summarize our findings and conclude.

II. ENTROPY REDUCTION IN A NON-UNITAL QUANTUM CHANNEL

We consider a single electron, our system, propagating through a reflectionless beam splitter and interacting with a localized quantum spin assuming the role of the micro environment, see Fig. (2) (in more general terms, this can be viewed as a flying system-qubit interacting with a environment-qubit). Our goal is to find a simple realization of a non-unital quantum channel that decreases the system's entropy when propagating from the input to the output leads. The interaction between the electron and the spin is mediated through the magnetic field generated by the electron's motion. An electron propagating through the lead α induces a unitary rotation $\hat{u}_\alpha$ of the spin. The electron scattering is described by the unitary scattering matrix $\hat{s}$, $|\beta\rangle = \sum_\alpha s_{\beta\alpha}|\alpha\rangle$, where $|\alpha\rangle$ describes the localized electron wave-packet moving in the incoming ($\alpha = 1, 2$) or outgoing ($\beta = 3, 4$) leads of the beam splitter. The incoming leads are defined by the electron's incoming state and are clearly distinguished from the outgoing state through the reflectionless property of the beam splitter.

We assume an initial state of the grand system 'electron plus spin' in a product form $\hat{R} = \hat{\rho} \otimes \hat{r}$, with the initial density matrices of the electron $\hat{\rho} = \sum_{\alpha\alpha'} \rho_{\alpha\alpha'} |\alpha\rangle\langle\alpha'|$ and the spin $\hat{r}$ to be determined. After the scattering, the density matrix of the grand system has the form

$$\mathcal{D}\hat{R} = \sum_{\alpha\alpha'\beta\beta'} s_{\beta\alpha}\rho_{\alpha\alpha'}s^*_{\beta'\alpha'}\, |\beta\rangle\langle\beta'| \otimes \left[\hat{u}_\beta \hat{u}_\alpha\, \hat{r}\, \hat{u}^\dagger_{\alpha'} \hat{u}^\dagger_{\beta'}\right] \quad (1)$$

and the resulting density matrix of the electron, $\mathcal{D}\hat{\rho} = {\rm Tr}_{\rm env}\{\mathcal{D}\hat{R}\}$, is given by

$$[\mathcal{D}\rho]_{\beta\beta'} = \sum_{\alpha\alpha'} s_{\beta\alpha}\rho_{\alpha\alpha'}s^*_{\beta'\alpha'}\, {\rm Tr}_{\rm env}\{\hat{r}\, \hat{u}^\dagger_{\alpha'}\hat{u}^\dagger_{\beta'}\hat{u}_\beta\hat{u}_\alpha\}. \quad (2)$$

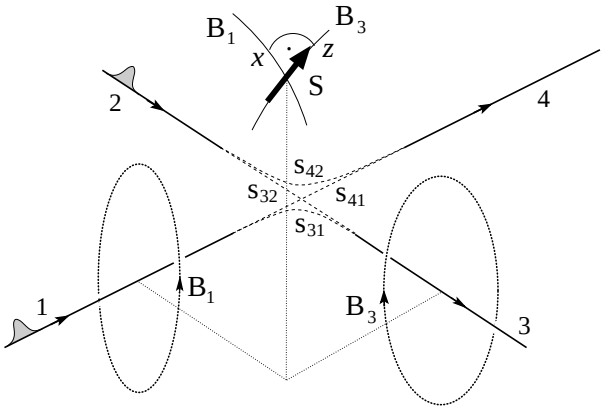

FIG. 2: Non-unital quantum channel realizing maximal purification by two consecutive orthogonal rotations $\hat{u}_1 = \sigma_x$ and $\hat{u}_3 = \sigma_z$. The 3D sketch illustrates the scattering of an electron incident from leads 1 and 2 and scattered into the leads 3 and 4; s_{ij} denote the scattering amplitudes. The micro-environment is defined through the spin $\mathbf{S}$ which interacts with the magnetic fields $\mathbf{B}$ generated by the electron travelling in the close-by leads 1 (generating the field $\mathbf{B}_1$) and 3 (generating the field $\mathbf{B}_3$); we ignore the interaction with currents in the distant leads 2 and 4. The geometry of the leads and the spin position is chosen such that the magnetic fields of the currents in leads 1 and 3 are orthogonal. The initial (or operational) spin states $|\uparrow\rangle$ and $|\downarrow\rangle$ are chosen parallel to z (the field generated by a current in lead 3) such that the passage of the electron in lead one flips the spin and generates the unitary $\hat{u}_1$. The passage of the electron through the lead 3 induces a rotation around z and adds the phases as required for the unitary $\hat{u}_3$.

The transformation $\mathcal{D}$ of the electron density matrix defined in Eq. (2) defines a quantum channel Φ. In the absence of an external magnetic field, the electron and spin do not exchange energy, i.e., the electron represents a thermodynamically isolated system in the classical sense. In order to discuss the unitality of this quantum channel, we analyse the evolution of the electron's chaotic quantum state $[\hat{\rho}_c]_{\alpha\alpha'} = \delta_{\alpha\alpha'}/2$ (or short $\hat{\rho}_c = \mathbb{1}/2$) which assumes the form

$$\Phi(\rho_c) = \mathcal{D}\rho_c = \frac{1}{2}\begin{pmatrix} 1 & \gamma \\ \gamma^* & 1 \end{pmatrix}, \tag{3}$$

where $\gamma = s_{31}s_{41}^*\mathrm{Tr}\{\hat{r}\,[\hat{u}_1^\dagger\hat{u}_4^\dagger\hat{u}_3\hat{u}_1 - \hat{u}_2^\dagger\hat{u}_4^\dagger\hat{u}_3\hat{u}_2]\}$ and the electron's entropy gain is given by $\Delta S(\hat{\rho}) = S(\mathcal{D}\hat{\rho}) - S(\hat{\rho}) = -[(1+|\gamma|)\ln(1+|\gamma|) + (1-|\gamma|)\ln(1-|\gamma|)]/2$. The entropy gain is negative and assumes its absolute maximal value $\ln 2$ at $|\gamma| = 1$. This value indeed can be realized for a specific choice of the device parameters. First, the maximum value of $|s_{31}s_{41}^*|$ is $1/2$ and requires a symmetric beam splitter. Next, we assume that the electron interacts with the spin only if it propagates in the bottom leads 1 and 3. Then,

$$|\gamma| = \left|\mathrm{Tr}\{\hat{r}\,[\hat{u}_1^\dagger\hat{u}_3\hat{u}_1 - \hat{u}_3]\}/2\right| \tag{4}$$

and its non-vanishing requires non-commuting spin rotations $\hat{u}_1$ and $\hat{u}_3$. The maximal value of $|\gamma| = 1$ is attained if there is a pure spin state $\hat{r} = |\uparrow\rangle\langle\uparrow|$ for which the unitary operations $\hat{u}_1$ and $\hat{u}_3$ satisfy the two conditions $\langle\uparrow|\hat{u}_1^\dagger\hat{u}_3\hat{u}_1|\uparrow\rangle = e^{i\phi}$ and $\langle\uparrow|\hat{u}_3|\uparrow\rangle = -e^{i\phi}$ with an arbitrary phase ϕ. The second condition requires that $\hat{u}_3|\uparrow\rangle = -e^{i\phi}|\uparrow\rangle$ (and $\hat{u}_3|\downarrow\rangle = e^{i\phi}|\downarrow\rangle$ when choosing $\hat{r} = |\downarrow\rangle\langle\downarrow|$, see below). In analyzing the first condition, we start with a general ansatz for $\hat{u}_1$, $\hat{u}_1|\uparrow\rangle = a|\uparrow\rangle + b|\downarrow\rangle$ with $|a|^2 + |b|^2 = 1$. The first condition requires that $\langle\uparrow|\hat{u}_1^\dagger\hat{u}_3\hat{u}_1|\uparrow\rangle = -|a|^2e^{i\phi} + |b|^2e^{i\varphi} = e^{i\phi}$ and hence $a = 0$, $e^{i(\phi-\varphi)} = 1$. We thus arrive at the following constraints for the unitary operations $\hat{u}_1$ and $\hat{u}_3$ that maximize $|\gamma|$,

$$\hat{u}_1|\uparrow\rangle = e^{i\alpha}|\downarrow\rangle, \qquad \hat{u}_1|\downarrow\rangle = e^{i\beta}|\uparrow\rangle, \tag{5}$$

$$\hat{u}_3|\uparrow\rangle = -e^{i\phi}|\uparrow\rangle, \quad \hat{u}_3|\downarrow\rangle = e^{i\phi}|\downarrow\rangle, \tag{6}$$

where $|\uparrow\rangle$ and $|\downarrow\rangle$ are some orthogonal spin states and ϕ, α, and β are arbitrary parameters. The conditions (5) and (6) mutually define the operational states $|\uparrow\rangle$ and $|\downarrow\rangle$ and one easily checks that $\gamma = 2s_{31}s_{41}^*e^{i\phi}$. A similar outcome with maximal $|\gamma| = 1$ but reversed sign $\gamma = -2s_{31}s_{41}^*e^{i\phi}$ appears when the spin is prepared in the orthogonal pure state $\hat{r} = |\downarrow\rangle\langle\downarrow|$. As a consequence, although the matrix element $\langle\downarrow|\hat{u}_1^\dagger\hat{u}_3\hat{u}_1 - \hat{u}_3|\uparrow\rangle = 0$ vanishes, a general superposition state $a|\uparrow\rangle + b|\downarrow\rangle$ of the qubit *does not* satisfy the condition $|\gamma| = 1$; e.g., a balanced superposition with $|a|^2 = |b|^2 = 1/2$ will reproduce the chaotic state with $\gamma = 0$. A possible geometry that implements this quantum channel is sketched in Fig. 2.

Hence, the above autonomous interaction of the electron residing in the fully chaotic state $\hat{\rho}_c$ and the spin prepared in either of the pure states $|\uparrow\rangle$ or $|\downarrow\rangle$ leads to a final electron state with vanishing entropy, i.e., the state of the system (the electron) is purified by the spin. Furthermore, with the electron appearing in a pure state after the transformation, the overall 'electron plus spin' state factorizes. Since the entropy of the grand system is conserved, the initial electron's entropy is absorbed by the spin, with the latter appearing in the fully chaotic state after the interaction with the electron.

Next, we generalize the observation that our spin-augmented scattering process exchanges a fully chaotic system state with the spin's pure states $|\uparrow\rangle$ or $|\downarrow\rangle$ to the cases of arbitrary pure and mixed initial system states as well as mixtures of $|\uparrow\rangle$ and $|\downarrow\rangle$ spin-states—note that this list is exhaustive, i.e., superpositions of $|\uparrow\rangle$ and $|\downarrow\rangle$ spin-states or even mixtures of such superpositions are not allowed. This analysis will demonstrate that our spin-augmented scattering setup acts as an autonomous quantum Maxwell demon with specific capabilities of exchanging states between the system and the micro-environment.

First, consider the transformation of a pure initial electron state. It is convenient to introduce the notation $|1\rangle = |\Uparrow\rangle$ and $|2\rangle = |\Downarrow\rangle$ for the incoming states. Similarly, we use the notation $|3\rangle = |\Uparrow\rangle$ and $|4\rangle = |\Downarrow\rangle$ for the outgoing leads in our reflectionless scatterer and keep in mind

that we switch the meaning of the $|\Uparrow\rangle$ and $|\Downarrow\rangle$ states when going from incoming to outgoing leads. We choose a symmetric beam splitter in the most general form,

$$\hat{s}(\theta,\eta) = \begin{pmatrix} s_{31} & s_{32} \\ s_{41} & s_{42} \end{pmatrix} = \frac{1}{\sqrt{2}} \begin{pmatrix} e^{i\theta} & -e^{-i\eta} \\ e^{i\eta} & e^{-i\theta} \end{pmatrix}. \quad (7)$$

Then, an arbitrary incoming state $|\phi_0\rangle = a|\Uparrow\rangle + b|\Downarrow\rangle$ of the electron experiences the transformation

$$\begin{aligned} |\phi_0\rangle\otimes|\uparrow\rangle \rightarrow \quad & |\Uparrow_{xy}\rangle\otimes\left[ae^{i\alpha}|\downarrow\rangle + be^{-i(\eta+\theta)}|\uparrow\rangle\right], \quad (8)\\ |\phi_0\rangle\otimes|\downarrow\rangle \rightarrow -&|\Downarrow_{xy}\rangle\otimes\left[be^{-i(\eta+\theta)}|\downarrow\rangle + ae^{i\beta}|\uparrow\rangle\right], \end{aligned}$$

where

$$\begin{aligned} |\Uparrow_{xy}\rangle &= \frac{e^{i(\phi+\theta)}|\Uparrow\rangle + e^{i\eta}|\Downarrow\rangle}{\sqrt{2}}, \quad (9)\\ |\Downarrow_{xy}\rangle &= \frac{e^{i(\phi+\theta)}|\Uparrow\rangle - e^{i\eta}|\Downarrow\rangle}{\sqrt{2}}, \end{aligned}$$

denote pure system states polarized within the equatorial xy-plane of the pseudo-spin states $|\Uparrow\rangle$ and $|\Downarrow\rangle$ and the final state of the spin is uniquely defined by the initial state $|\phi_0\rangle$ of the electron/system.

In both cases, chaotic or pure initial system states, the final state of the grand system (electron plus qubit) is again a product state, provided that the qubit was initially prepared in one of the specific operating states $|\uparrow\rangle$ or $|\downarrow\rangle$ defined the by electron–qubit interaction, see Eqs. (5) and (6). Moreover, the final states $|\Uparrow_{xy}\rangle$ and $|\Downarrow_{xy}\rangle$ of the electron do not depend on its initial state $|\phi_0\rangle$ and are determined only by the initial state of the qubit, by the parameters (θ,η) of the beam splitter, and by the interaction phase ϕ. The additional phases α and β appearing in the definition of $\hat{u}_1$, Eq. (5), show up only in the final qubit state.

In a more general situation, the initial states of both the system as well as the spin qubit can be mixed. We start with the qubit in an incoherent mixture of the $|\uparrow\rangle$ and $|\downarrow\rangle$ states, $\hat{r} = p_+|\uparrow\rangle\langle\uparrow| + p_-|\downarrow\rangle\langle\downarrow|$ and the electron in a mixed state $\hat{\rho}$ written in the diagonal representation $\hat{\rho} = p_1|\phi_1\rangle\langle\phi_1| + p_2|\phi_2\rangle\langle\phi_2|$ with $|\phi_j\rangle = a_j|\Uparrow\rangle + b_j|\Downarrow\rangle$ and $\langle\phi_1|\phi_2\rangle = 0$. Then, according to Eq. (8), the initial product state $\hat{R} = \hat{\rho}\otimes\hat{r}$ transforms into the sum of product states

$$\mathcal{D}\hat{R} = p_+|\Uparrow_{xy}\rangle\langle\Uparrow_{xy}|\otimes\hat{r}_+ + p_-|\Downarrow_{xy}\rangle\langle\Downarrow_{xy}|\otimes\hat{r}_-, \quad (10)$$

where the final density matrices of the qubit $\hat{r}_\pm = p_1|\psi_{\pm1}\rangle\langle\psi_{\pm1}| + p_2|\psi_{\pm2}\rangle\langle\psi_{\pm2}|$ are defined by the initial states of the electron, $|\psi_j\rangle = b_je^{-i(\eta+\theta)}|\uparrow\rangle + a_je^{i\alpha}|\downarrow\rangle$, $|\psi_{-j}\rangle = a_je^{i\beta}|\uparrow\rangle + b_je^{-i(\eta+\theta)}|\downarrow\rangle$.

Comparing initial and final states in (10), one notes that the electron and spin have swapped their initial entropies. The most extreme case is given by an electron incoming in the chaotic state $\hat{\rho} = \mathbb{1}/2 = \left(|\Uparrow\rangle\langle\Uparrow| + |\Downarrow\rangle\langle\Downarrow|\right)/2$ with maximal entropy $k_{\rm B}\ln 2$ and the qubit in one of the pure states $|\uparrow\rangle$ or $|\downarrow\rangle$. Then, the product state of the grand system, e.g., $\hat{R} = \mathbb{1}/2\otimes|\uparrow\rangle\langle\uparrow|$, is transformed into the new product state $\mathcal{D}\hat{R} = |\Uparrow_{xy}\rangle\langle\Uparrow_{xy}|\otimes\mathbb{1}/2$ with the electron residing in the pure state $|\Uparrow_{xy}\rangle$. Hence, our qubit-assisted scattering setup acts as an autonomous quantum Maxwell demon, with the electron's original entropy $k_{\rm B}\ln 2$ completely transferred to the spin qubit, as the latter ends up in the chaotic state. We thus call the auxiliary spin-qubit our 'purifying' or 'demon' qubit. Note that this transfer of entropy does not involve any transfer of energy, nor is there an external supply of energy during the process.

However, the above exchange of entropy holds true only if the demon qubit has been initially prepared in either of the pure states $|\uparrow\rangle$ or $|\downarrow\rangle$ or an incoherent mixture thereof. For such a specific preparation of the demon, the entropy of the system is reduced if the initial state of the demon is more pure than the one of the system. In the more general situation where the initial state of the demon is a superposition state of $|\uparrow\rangle$ and $|\downarrow\rangle$ or an arbitrary mixed state, the above scheme does not lead to an entropy exchange between the two subsystems. Thus, although our process does not require knowledge about the initial system state, it does require a proper preparation of the demon qubit.

III. IMPOSED COHERENCE ON A FLYING QUBIT

We now study a scattering electron within an alternative setup where the spin defining the micro-environment is replaced by a tunable quantum double-dot with degenerate states,

$$\hat{H}_0 = \epsilon_0\left[\,|\uparrow_z\rangle\langle\uparrow_z| + |\downarrow_z\rangle\langle\downarrow_z|\,\right] - \left[\,\Delta(t)\,|\uparrow_z\rangle\langle\downarrow_z| + \text{h.c.}\,\right], \quad (11)$$

i.e., the two dots constituting the qubit have equal energies ϵ_0 (we assume $\epsilon_0 = 0$ from now on). The tunneling amplitude $\Delta(t) \equiv |\Delta(t)|e^{i\varphi}$ between the dots can be dynamically changed, see below. The dynamics of the flying qubit is still described by the scattering matrix Eq. (7). This setup appears simpler to realize, with the action of the micro-environment involving equal operations before and after the scattering event. The price to pay then is an additional basis change (or rotation) of the double-dot qubit in between the two interaction events.

Consider an electron wave packet (our system) which propagates through the edge states of an Integer Quantum Hall bar device and which scatters at a quantum point contact (QPC), see Fig. 3. The electron arrives at the QPC through the incoming edge channels $|0,+\rangle$ and $|1,-\rangle$ and scatters into the outgoing leads $|0,-\rangle$ and $|1,+\rangle$. It is convenient to use the pseudo-spin notation $|0,+\rangle = |\Uparrow\rangle$ and $|1,-\rangle = |\Downarrow\rangle$ for the incoming states and the same for the outgoing ones, $|0,-\rangle = |\Uparrow\rangle$ and $|1,+\rangle = |\Downarrow\rangle$, while keeping in mind to switch meaning when going from incoming to outgoing leads. The elastic scattering process is described by a symmetric scattering matrix $\hat{s}(\theta,\eta)$, see Eq. (7). The micro-environment interacting with the scattering electron is given by a double-

dot, replacing the spin-environment in the previous section. We use the spin notation $|\uparrow_z\rangle$ ($|\downarrow_z\rangle$) to describe the double-dot's semi-classical state with a localized charge in the right (left) dot of the qubit.

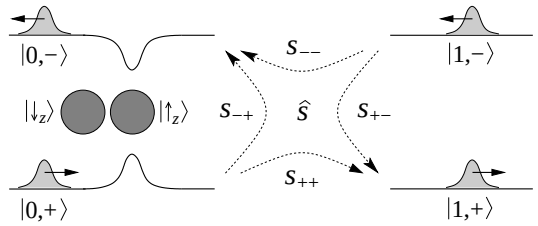

FIG. 3: An electron in an incoming superposition state $a|0,+\rangle + b|1,-\rangle$ undergoes scattering in a quantum point contact (a QPC, here implemented in a Quantum Hall bar device) described by the scattering matrix $\hat{s}$ with symmetric scattering coefficients s_{ij}, $i,j = \pm$. The states $|0,\pm\rangle$ interact with a double dot residing in one of the operational states $|\uparrow\rangle$ or $|\downarrow\rangle$ which are superpositions of the physical states $|\uparrow_z\rangle$ and $|\downarrow_z\rangle$. The interaction between the double-dot and the scattering states $|0,\pm\rangle$ generates the conditional (on $|\Uparrow\rangle$) π-phase shift $\hat{u}$. Combining this operation with the scattering of the electron at the QPC and a $\pi/2$-rotation of the double-dot, see text, swaps the electron and double-dot states.

We place the charge qubit to the left of the QPC such that it interacts capacitively and symmetrically with the electron propagating in either of the two left leads $|\Uparrow\rangle$ (i.e., both $|0,\pm\rangle$), while leaving the right leads $|\Downarrow\rangle$ invariant. Our task is to find an interaction and an operational basis $|\uparrow\rangle$ and $|\downarrow\rangle$ that satisfy the conditions (5) and (6). The latter tell, that $\hat{u}_3$ shall add a phase difference of π to the operational states and $\hat{u}_1$ shall exchange them. The electron–qubit interaction acts on the physical qubit states $|\uparrow_z\rangle$ and $|\downarrow_z\rangle$, provided the electron passes the double-dot in a $|\Uparrow\rangle$ state. We then can use the interaction to generate the relative phase shift π, e.g., by placing the two dots in a symmetric manner between the left incoming and outgoing wires and choosing a geometry that couples one of the dots more strongly to the leads, see Fig. 3. Hence, we demand that the electron–qubit interaction shall generate the unitary transformation (a rotation around the z-axis)

$$\begin{aligned}
\hat{U}|\Uparrow\rangle\otimes|\uparrow_z\rangle &= \quad e^{i\phi}|\Uparrow\rangle\otimes|\uparrow_z\rangle, \\
\hat{U}|\Uparrow\rangle\otimes|\downarrow_z\rangle &= -e^{i\phi}|\Uparrow\rangle\otimes|\downarrow_z\rangle, \\
\hat{U}|\Downarrow\rangle\otimes|\uparrow_z\rangle &= |\Downarrow\rangle\otimes|\uparrow_z\rangle, \\
\hat{U}|\Downarrow\rangle\otimes|\downarrow_z\rangle &= |\Downarrow\rangle\otimes|\downarrow_z\rangle.
\end{aligned} \tag{12}$$

We have used a capital letter $\hat{U}$ to denote the operator acting on the grand system. The action of $\hat{U}$ on the joint system then corresponds to a controlled (relative) phase shift.

However, according to (6) it is the operational states $|\uparrow\rangle$ and $|\downarrow\rangle$ that should pick up this relative phase; furthermore, the latter should be flipped by the operation $\hat{u}_1$. Hence, we should introduce a $\pi/2$ rotation that transforms between planar operational states $|\uparrow\rangle$ and $|\downarrow\rangle$ and axial physical states $|\uparrow_z\rangle$ and $|\downarrow_z\rangle$.

In order to rotate the qubit state, we tune the tunneling amplitude $\Delta(t) \equiv |\Delta(t)|e^{i\varphi}$ in Eq. (11). Assuming a finite but constant $\Delta(t)$, the evolution of the qubit is described by the unitary operator $\hat{u}(\tau) = \exp(-i\hat{H}_0\tau/\hbar)$. In particular, we consider the specific unitary transformation $\hat{u}_{1/4} \equiv \hat{u}(\tau_{1/4})$ for a fixed time interval $\tau_{1/4} = \hbar\pi/4|\Delta|$,

$$\hat{u}_{1/4} = \frac{1}{\sqrt{2}}\begin{pmatrix} 1 & ie^{i\varphi} \\ ie^{-i\varphi} & 1 \end{pmatrix}, \tag{13}$$

that rotates the physical states $|\uparrow_z\rangle$ and $|\downarrow_z\rangle$ into the xy-plane. Defining the operational states

$$\begin{aligned}
|\uparrow\rangle &= \hat{u}_{1/4}|\uparrow_z\rangle, \\
|\downarrow\rangle &= \hat{u}_{1/4}|\downarrow_z\rangle,
\end{aligned} \tag{14}$$

the electron–qubit interaction in Eq. (12) acts on the demon states with the following unitary

$$\begin{aligned}
\hat{u}\,|\uparrow\rangle &= -ie^{i(\phi-\varphi)}|\downarrow\rangle, \\
\hat{u}\,|\downarrow\rangle &= \quad ie^{i(\phi+\varphi)}|\uparrow\rangle,
\end{aligned} \tag{15}$$

which is equivalent to the action of the $\hat{u}_1$ operator, see Eq. (5) with $\alpha = \phi - \varphi - \pi/2$ and $\beta = \phi + \varphi + \pi/2$, i.e., $\hat{u} = \hat{u}_1(\alpha,\beta)$. On the other hand, we can implement the simple phase shift operation of $\hat{u}_3$, see Eq. (6), by rotating the operational state back to the physical state and let the interaction act with the transformation $\hat{u}$ once more. The transformation between the operational $|\uparrow\rangle, |\downarrow\rangle$ and the physical $|\uparrow_z\rangle, |\downarrow_z\rangle$ basis states is given by $\hat{u}_{1/4}$, the unitary gate in Eq. (13) which is written in the physical $|\uparrow_z\rangle, |\downarrow_z\rangle$ basis. Expressing the operational basis through the physical one, $|\uparrow\rangle = \big[|\uparrow_z\rangle + ie^{-i\varphi}|\downarrow_z\rangle\big]/\sqrt{2}$ and $|\downarrow\rangle = \big[ie^{i\varphi}|\uparrow_z\rangle + |\downarrow_z\rangle\big]/\sqrt{2}$, one finds that $\hat{u}_{1/4}|\uparrow\rangle = ie^{-i\varphi}|\downarrow_z\rangle$ and $\hat{u}_{1/4}|\downarrow\rangle = ie^{i\varphi}|\uparrow_z\rangle$, and hence

$$\begin{aligned}
\hat{u}^\dagger_{1/4}\hat{u}\,\hat{u}_{1/4}|\uparrow\rangle &= -e^{i\phi}|\uparrow\rangle, \\
\hat{u}^\dagger_{1/4}\hat{u}\,\hat{u}_{1/4}|\downarrow\rangle &= \quad e^{i\phi}|\downarrow\rangle,
\end{aligned} \tag{16}$$

i.e., $\hat{u}^\dagger_{1/4}\hat{u}\,\hat{u}_{1/4} = \hat{u}_3$. We conclude that in the present setup, the two non-commuting unitary operations $\hat{u}_1$ and $\hat{u}_3$ can be realized by letting the electron and the double-dot interact twice in the same manner, once in the incoming and a second time in the outgoing lead, provided that the qubit is rotated by $\hat{u}_{1/4}$ between the two interaction events (note that the last single-qubit rotation $\hat{u}^\dagger_{1/4}$ can be dropped). For an electron wavepacket with a finite width, the interaction with the double-dot has to be separated in time from the subsequent scattering at the QPC. The evolution of the overall system then can be separated into four steps, i) preparation: starting with a physical (localized) state $|\uparrow_z\rangle$ or $|\downarrow_z\rangle$, the tunneling Δ is switched on during the time $\tau_{1/4}$ in order to generate the operational states $|\uparrow\rangle$ and $|\downarrow\rangle$. ii) first interaction:

the electron interacts with the double-dot in the incoming lead, thereby generating the transformation $\hat{u} = \hat{u}_1$. iii) single-qubit rotations: while the electron undergoes scattering at the QPC, the double-dot is rotated by $\hat{u}_{1/4}$ (by again switching on the tunneling Δ during the time $\tau_{1/4}$) as part of the $\hat{u}_3$ operation. iv) second interaction: the electron interacts with the double-dot in the outgoing lead as part of the $\hat{u}_3$ transformation. As we can drop the last qubit rotation $\hat{u}_{1/4}^\dagger$ this completes the sequence. The above evolution transforms any initial electron (or flying qubit) state $|\phi_0\rangle = a\,|\Uparrow\rangle + b\,|\Downarrow\rangle$ into the pure planar states $|\Uparrow_{xy}\rangle$ or $|\Downarrow_{xy}\rangle$ as given in Eq. (9). Keeping $\Delta = 0$ during the process (except for the time intervals during the demon rotations) the above evolution occurs without energy exchange between the electron and the double dot. Thus, the described protocol produces the same energy-conserving non-unital quantum channel as described in the previous section but requires an external manipulation of the demon qubit between the two interaction events.

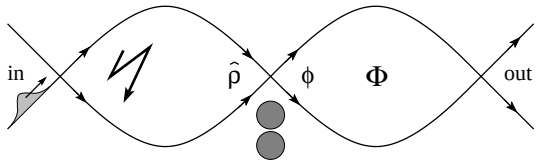

FIG. 4: Schematic version of a double Mach-Zehnder Interferometer with quantum demon. The incoming wave-packet is decohered (arrow) in the first loop and restored to a pure state $|\phi\rangle$ by the action of the demon (double-dot). The second loop tests the coherence of the wave function by shifting the relative phase in the two arms with the help of a tunable flux Φ. The appearance of Aharonov-Bohm oscillations in the outgoing arms testifies for the successful action of the demon.

The functionality of the demon's purification action can be experimentally demonstrated in a mesoscopic quantum interference setting as sketched in Fig. 4. To this end, we consider two consecutive Mach-Zehnder interferometers where the electron first looses its coherence within the first loop through a dephasing process, e.g., via entanglement with another qubit. The electron then arrives at the intermediate QPC in a mixed state (manifest after tracing out the entangled qubit). The demon-enhanced QPC operating with a pure demon qubit then restores the purity of the electron state, what can be observed in the resurrection of Aharonov-Bohm oscillations in the outgoing leads of the second interferometer as the flux Φ penetrating the second loop is varied. Furthermore, replacing the demon's qubits by mixed states, these Aharonov-Bohm oscillations can be tuned with a visibility changing between one and zero.

The Mach-Zehnder setup motivates a yet other formulation of the demon's functionality. Injecting an electron (1) into the first loop, entangling it with a dephasing qubit (2), and performing the demon's action involving the demon qubit (3) swaps the entanglement between (1) and (2) to the entanglement between (2) and (3), letting (1) further evolve in a pure state. Note that while a direct measurement of entropy reduction is difficult, the observation of increased visibility in a Mach-Zehnder device due to improved coherence offers an attractive substitute.

Also, it is interesting to compare the different functionalities of classical and quantum Maxwell demons. In the above setup, the action of the quantum demon generates a prescribed electronic quantum state in the second interferometer. A corresponding classical demon[17] achieving this task would first measure the electron's state in the first interferometer and, depending on the measurement outcome (upper or lower lead), adjust the scattering matrix $\hat{s}$ in such a way as to produce the desired quantum state in the second interferometer through the scattering process. The notion 'classical' then refers to the demon's property to acquire classical information on the system. The functionalities of the two schemes are very different: the classical Maxwell demon interrupts the quantum evolution of the system by measuring its quantum state. The obtained classical information is subsequently used in a conditional manipulation of the system. The action of the quantum Maxwell demon is conceptually different: the system's quantum evolution is never interrupted and the evolution of the joint system–demon setup is autonomous. Furthermore, although the quantum demon acquires the initially unknown system state, see Eq. (8), no use is made of this information in the process; in fact, this information is discarded after the pSWAP operation. Instead, it is the known quantum state stored in the demon and later deposited into the system that is relevant for the functionality of the process. Hence, while the classical Maxwell demon *acquires* some classical information about the system's state, our quantum Maxwell demon *places* some known quantum state into the system.

In this context, we also refer to the analysis in Ref. [23] where the action of a classical Maxwell demon was included in the entropy balance of the system by introducing the *mutual information* $I_{\mathcal{S};\mathcal{D}} \geq 0$ quantifying the information stored in the demon about the system. The Second Law as applied to the system alone then has to be extended[23] to include this mutual information, $\Delta S_{\mathcal{S}} + I_{\mathcal{S};\mathcal{D}} \geq 0$. The inequality tells that the information on the system learnt by the demon can be used to reduce the system's entropy by the maximal amount $\Delta S_{\mathcal{S}} = -I_{\mathcal{S};\mathcal{D}}$. It is important to distinguish this classical type of entropy decrease from our quantum process. The literal application of the analysis in Ref. [23] to our quantum setup cannot explain its entropy decrease in the scattering process: since the flying and demon qubits start out and end up in a product state before and after the scattering, we have $I_{\mathcal{S};\mathcal{D}} = 0$ and hence the classical expectation is that $\Delta S_{\mathcal{S}} \geq 0$, in obvious conflict with our entropy decrease due to the pSWAP.

IV. QUANTUM CIRCUIT DESCRIPTION

The demon's action can be conveniently formalized in the quantum circuit language. Indeed, each stage of the system–demon evolution can be described by a corresponding quantum gate. We choose the product basis $\{|\Uparrow\rangle, |\Downarrow\rangle\} \otimes \{|\uparrow\rangle, |\downarrow\rangle\}$ as our representation of the initial joint system state and the product basis $\{|\Uparrow\rangle, |\Downarrow\rangle\} \otimes \{|\uparrow\rangle, |\downarrow\rangle\}$ as our representation of the final joint system state and use lower case (capital) letters to denote operators acting on the individual (joint) system. Below we consider a specific situation with the interaction phase $\phi = 0$ and the tunneling phase $\varphi = -\pi/2$, implying $\alpha = 0$ and $\beta = 0$. Then the unitary rotation $\hat{u}$ induced by the electron–qubit interaction as described in Eq. (15) corresponds to a CNOT quantum gate when extended to the joint electron–demon system, $\hat{U} = \mathrm{CNOT}_{\mathrm{d}}^{\mathrm{s}\Uparrow}$, where the electron or system state serves as the control, $\hat{U}(|\Uparrow\rangle \otimes |\uparrow\rangle) = |\Uparrow\rangle \otimes |\downarrow\rangle$ and $\hat{U}(|\Uparrow\rangle \otimes |\downarrow\rangle) = |\Uparrow\rangle \otimes |\uparrow\rangle$, while $\hat{U}(|\Downarrow\rangle \otimes |\uparrow\rangle) = |\Downarrow\rangle \otimes |\uparrow\rangle$ and $\hat{U}(|\Downarrow\rangle \otimes |\downarrow\rangle) = |\Downarrow\rangle \otimes |\downarrow\rangle$. In between the interaction events the evolution is described by two single-qubit rotations, one on the electron and another on the qubit. In the demon's operating basis, the qubit rotation $\hat{u}_{1/4}$ corresponds to a Hadamard-type gate, $\hat{u}_{1/4} = \sigma_z \mathrm{H} \equiv \bar{\mathrm{H}}$ with H the standard Hadamard operation, $\hat{u}_{1/4}|\uparrow\rangle = \big(|\uparrow\rangle - |\downarrow\rangle\big)/\sqrt{2}$ and $\hat{u}_{1/4}|\downarrow\rangle = \big(|\uparrow\rangle + |\downarrow\rangle\big)/\sqrt{2}$. The electron state is transformed according to the scattering matrix $\hat{s}(\theta, \eta)$ of the QPC; for the specific choice $\theta = 0$ and $\eta = \pi$ it can be represented by our Hadamard-type gate as well, $\hat{s}(0, \pi) = \bar{\mathrm{H}}$. Hence, the overall unitary transformation of the demon's purification protocol (expressed in the basis $\{|\Uparrow\rangle\otimes|\uparrow\rangle, |\Uparrow\rangle\otimes|\downarrow\rangle, |\Downarrow\rangle\otimes|\uparrow\rangle, |\Downarrow\rangle\otimes|\downarrow\rangle\}$) is

$$\hat{U}_{\mathcal{D}} = \mathrm{CNOT}_{\mathrm{d}}^{\mathrm{s}\Uparrow} \cdot \big[\bar{\mathrm{H}}_{\mathrm{s}} \otimes \bar{\mathrm{H}}_{\mathrm{d}}\big] \cdot \mathrm{CNOT}_{\mathrm{d}}^{\mathrm{s}\Uparrow} = \frac{1}{2}\begin{pmatrix} 1 & -1 & -1 & 1 \\ 1 & 1 & 1 & 1 \\ -1 & -1 & 1 & 1 \\ -1 & 1 & -1 & 1 \end{pmatrix}. \tag{17}$$

The simplest explicit form of the $\hat{U}_{\mathcal{D}}$ matrix is obtained when performing two additional Hadamard-type gates at the output of the circuit, $\hat{V}_{\mathcal{D}} = \big[\bar{\mathrm{H}}_{\mathrm{s}}^{-1} \otimes \bar{\mathrm{H}}_{\mathrm{d}}\big] \cdot \hat{U}_{\mathcal{D}}$ (see Fig. 5 for the corresponding quantum circuit diagram; note that the last rotation $\bar{H}_{\mathrm{d}}$ is not the rotation $\hat{u}_{1/4}^{\dagger}$ completing the operation $\hat{u}_3$ in (16)),

$$\hat{V}_{\mathcal{D}} = \big[\bar{\mathrm{H}}_{\mathrm{s}}^{-1} \otimes \bar{\mathrm{H}}_{\mathrm{d}}\big] \cdot \mathrm{CNOT}_{\mathrm{d}}^{\mathrm{s}\Uparrow} \cdot \big[\bar{\mathrm{H}}_{\mathrm{s}} \otimes \bar{\mathrm{H}}_{\mathrm{d}}\big] \cdot \mathrm{CNOT}_{\mathrm{d}}^{\mathrm{s}\Uparrow} = \begin{pmatrix} 1 & 0 & 0 & 0 \\ 0 & 0 & 1 & 0 \\ 0 & 0 & 0 & 1 \\ 0 & 1 & 0 & 0 \end{pmatrix}. \tag{18}$$

The operations $\hat{U}_{\mathcal{D}}$ and $\hat{V}_{\mathcal{D}}$ both describe the pSWAP operation of the demon and differ only by a final change of basis.

The operation $\hat{V}_{\mathcal{D}}$ acts as a SWAP only on one pair of basis states,

$$\hat{V}_{\mathcal{D}} |\Uparrow\rangle \otimes |\uparrow\rangle = |\Uparrow\rangle \otimes |\uparrow\rangle, \qquad \hat{V}_{\mathcal{D}} |\Downarrow\rangle \otimes |\uparrow\rangle = |\Uparrow\rangle \otimes |\downarrow\rangle, \tag{19}$$

while the second pair is swapped up to a NOT operation on the demon qubit,

$$\hat{V}_{\mathcal{D}} |\Uparrow\rangle \otimes |\downarrow\rangle = |\Downarrow\rangle \otimes |\downarrow\rangle, \qquad \hat{V}_{\mathcal{D}} |\Downarrow\rangle \otimes |\downarrow\rangle = |\Downarrow\rangle \otimes |\uparrow\rangle, \tag{20}$$

hence the name partial SWAP or pSWAP. Summarizing, the demon's operation $\hat{V}_{\mathcal{D}}$ swaps the system- and demon qubit states (up to an independent unitary rotation of each subsystem) if the demon qubit was initially prepared in a pure operational state $|\uparrow\rangle = (1, 0)$ or $|\downarrow\rangle = (0, 1)$, $\hat{V}_{\mathcal{D}}[(a, b) \otimes (1, 0)] = (1, 0) \otimes (a, b)$ and $\hat{V}_{\mathcal{D}}[(a, b) \otimes (0, 1)] = (0, 1) \otimes (b, a)$. However, for an arbitrary initial state of the qubit, the circuit does not operate as a SWAP gate, $\hat{V}_{\mathcal{D}}[(a, b) \otimes (\alpha, \beta)] \neq (\alpha, \beta) \otimes (a, b)$.

In order to arrive at a full SWAP operation, we have to add another CNOT operation which acts on the demon when the controlling system is in the $|\Downarrow\rangle$ state,

$$\mathrm{SWAP} = \mathrm{CNOT}_{\mathrm{d}}^{\mathrm{s}\Downarrow} \cdot \hat{V}_{\mathcal{D}} = \begin{pmatrix} 1 & 0 & 0 & 0 \\ 0 & 0 & 1 & 0 \\ 0 & 1 & 0 & 0 \\ 0 & 0 & 0 & 1 \end{pmatrix}. \tag{21}$$

However, such a gate would require a more sophisticated interaction that is not easily realized within our physical setting, while an implementation using spins and proper NMR sequences seems more promising[10]. The circuit diagram for the pSWAP and its extension to the SWAP operation are shown in Fig. 5.

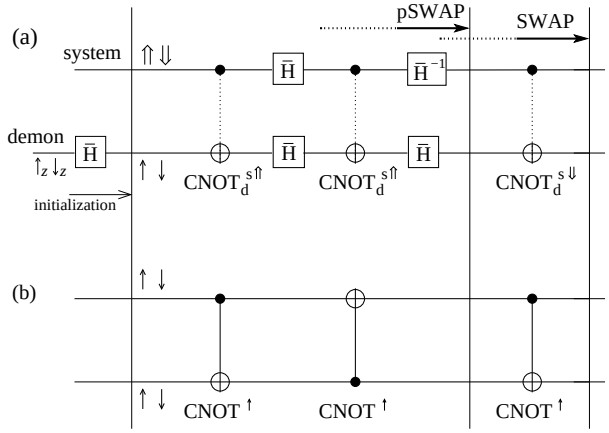

FIG. 5: (a) Quantum circuit describing the demon action as a partial SWAP or pSWAP and its extension to a full SWAP operation. The dotted lines on the CNOT operations indicate that no energy is exchanged between the system and demon qubits. (b) Minimal pSWAP and SWAP operations using two and three CNOT operations with exchanged controller[39].

V. QUANTUM THERMODYNAMIC ENGINE

The energy-conserving pSWAP operation invites the design of a quantum-thermodynamic engine[10,12,35] which transforms heat from a single reservoir into work (or ordered energy) by making use of quantum purity provided by a demon with energy-degenerate quantum states. The specific design of our machine naturally separates its operation into two cycles with no energy transfer across, one cycle providing energy or work from a single thermal reservoir, while the purification of the demon's qubits can be handled in a separate 'entropy cycle' away from the engine. This contrasts with the operation of a classical machine where the maximal extractable work is given by the Helmholtz free energy $\delta F = \delta U - T\delta S$ of the thermodynamic process[40] (the same holds for a class of quantum engines[7]), binding the energy and entropy flows in the process.

The engine consists of two (identical) working qubits (two two-level systems) with fixed energy-level spacing $\Delta_{\rm w}$ described by the Hamiltonian (note the correspondence $|g\rangle \leftrightarrow |\Downarrow\rangle$ and $|e\rangle \leftrightarrow |\Uparrow\rangle$)

$$\hat{H}_{\rm w} = \Delta_{\rm w}|e\rangle\langle e| \tag{22}$$

that can be coupled to a thermal reservoir at the temperature T. The system is enhanced by two demon qubits with degenerate levels as described by Eq. (11), see Fig. 6 for a sketch of this setup. We first analyse an idealized working cycle and discuss issues related with practical implementations later on.

The two working qubits (wits), assuming the role of the system qubits, start out in their ground states $|g\rangle \leftrightarrow |\Downarrow\rangle$ and then are placed into thermal contact with a macroscopic heat reservoir at a temperature T. After the isochoric thermalisation (i.e., the energy level spacing $\Delta_{\rm w}$ of the wits remains unchanged), both wits are detached from the heat reservoir; their states are described by the density matrices $\hat{\rho}_{\rm w} = Z^{-1}\exp(-\beta\hat{H}_{\rm w}) = p_g|g\rangle\langle g| + p_e|e\rangle\langle e|$, with $\beta = 1/T$ the inverse temperature (we set the Boltzmann constant to unity), $p_g = 1/Z$, $p_e = e^{-\beta\Delta_{\rm w}}/Z$, and $Z = 1 + e^{-\beta\Delta_{\rm w}}$.

Next, a modified p̃SWAP operation with a pair of demon qubits (dits) prepared in pure operational energy-degenerate states $\hat{r}_\uparrow = |\uparrow\rangle\langle\uparrow|$ and $\hat{r}_\downarrow = |\downarrow\rangle\langle\downarrow|$ exchanges wit and dit states,

$$\begin{aligned}\tilde{\rm pSWAP} = \big[\hat{u}_{1/4}\otimes \mathbb{1}\big]\cdot {\rm CNOT}_{\rm d}^{\rm w\Uparrow} \\ \cdot \big[\hat{u}_{1/4}\otimes \bar{\rm H}_{\rm d}\big]\cdot {\rm CNOT}_{\rm d}^{\rm w\Uparrow},\end{aligned} \tag{23}$$

where $\hat{u}_{1/4}$ is a Hadamard-type transformation of the working qubit, see Eq. (13). E.g., assuming an interaction between the wits and dits that generates a conditional π-shift as described in Eq. (12) with $\phi = 0$, we choose appropriate operational dit states $|\uparrow\rangle$ and $|\downarrow\rangle$ according to Eq. (14); this generates a ${\rm CNOT}_{\rm d}^{\rm w\Uparrow}$ operation that flips the dit when the wit is in the excited state. After the p̃SWAP operation, the two wit–dit systems reside in the states (we assume phases $\theta = \phi = 0$ and $\eta = \pi/2 - \varphi$)

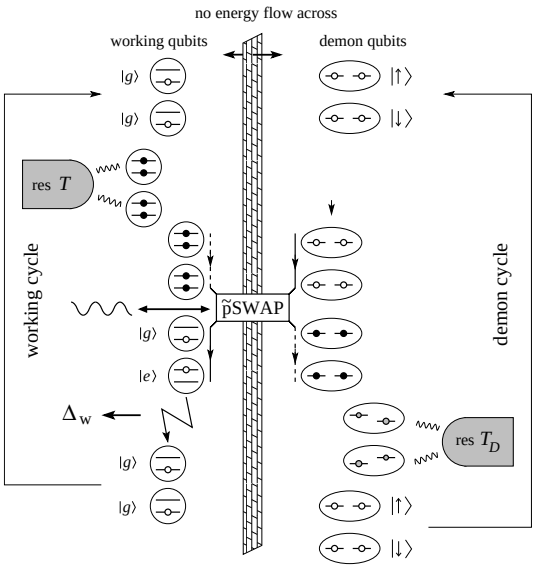

FIG. 6: Quantum thermodynamic engine with two energetically separated cycles. The working cycle (left) starts with two working qubits (wits) in the pure (empty dots) ground state $|g\rangle$. The contact with the thermal reservoir excites them into a mixed (solid dots) state. After the demon's swap, the wits have taken over the pure states from the demon qubits (dits), $|\uparrow\rangle \to |e\rangle$ and $|\downarrow\rangle \to |g\rangle$. The energy $\Delta_{\rm w}$ of the excited wit can be used for work extraction. Different from the pSWAP in Fig. 1, the present p̃SWAP has an energy context involving a classical field (wavy line). The entropy cycle (right) starts with two pure dits in states $|\uparrow\rangle$ and $|\downarrow\rangle$ which are 'consumed' by the wits and then reprepared for the next cycle.

$$\tilde{\rm pSWAP}\big[\hat{\rho}_{\rm w}\otimes\hat{r}_\uparrow\big] = \hat{\rho}_g\otimes\hat{r}_+, \tag{24}$$

$$\tilde{\rm pSWAP}\big[\hat{\rho}_{\rm w}\otimes\hat{r}_\downarrow\big] = \hat{\rho}_e\otimes\hat{r}_-, \tag{25}$$

where $\hat{\rho}_g = |g\rangle\langle g|$, $\hat{\rho}_e = |e\rangle\langle e|$ and $\hat{r}_+ = p_g|\uparrow\rangle\langle\uparrow| + p_e|\downarrow\rangle\langle\downarrow|$, $\hat{r}_- = p_g|\downarrow\rangle\langle\downarrow| + p_e|\uparrow\rangle\langle\uparrow|$ are final mixed states of the demon qubits, see Eq. (10). The net average energy cost of this pair of p̃SWAP operations is given by the difference of the final and initial average energy of the working qubits,

$$W_- = \Delta_{\rm w} - 2p_e\Delta_{\rm w} = \Delta_{\rm w}\,\frac{1-e^{-\beta\Delta_{\rm w}}}{1+e^{-\beta\Delta_{\rm w}}}. \tag{26}$$

The p̃SWAP operation deterministically pushes the first wit into the ground state and the second wit into its excited state. The latter now stores an ordered energy (or work) $W_+ = \Delta_{\rm w}$ which can be extracted, e.g., with the help of a half-Rabi pulse $\hat{u}_{1/2}|e\rangle = \hat{u}_{1/4}\hat{u}_{1/4}|e\rangle = ie^{-i\varphi}|g\rangle$ of coherent radiation. Calculating the energy balance of the working cycle, one finds that this cycle operates with unit efficiency $\eta = 1$, as all of the initial heat $Q = 2p_e\Delta_{\rm w}$ stored in the two wits is transformed into net useful work $W_{\rm out} = W_+ - W_- = Q$ in a deterministic fashion. The entropy increase of the wits due to the isochoric heating

is absorbed by the dits with no additional energy cost, resulting in the above unit efficiency for the heat-to-work conversion in a single cycle. In order to do so, the working cycle consumes the purity provided by the two energy-degenerate demon qubits and we will discuss the cost of this consumption below.

In the sequence Eq. (23), the two transformations $\hat{u}_{1/4}$ on the wits require an external supply of work[41] since they transform between the pure-energy wit mixtures of $|g\rangle$ and $|e\rangle$ and the balanced superposition states $|s_1\rangle = [ie^{i\varphi}|e\rangle + |g\rangle]/\sqrt{2}$ and $|s_2\rangle = [|e\rangle + ie^{-i\varphi}|g\rangle]/\sqrt{2}$. This process requires an external work $\Delta_{\rm w}/2$ or $-\Delta_{\rm w}/2$ to be provided to or extracted from the working qubits (the final $\hat{u}_{1/4}$ operation transforms the superpositions $|s_1\rangle$ and $|s_2\rangle$ into the pure-energy states $|g\rangle$ and $|e\rangle$). For a pair of wits in fully chaotic states, the combination of these operations does not involve a net *average* energy transfer between the field and the qubits and hence does not require an external flow of energy. This (at least on average) energy conservation is due to our use of two demon qubits residing in opposite states $|\uparrow\rangle$ and $|\downarrow\rangle$: while the demon qubit in state $|\downarrow\rangle$ always generates a wit in the excited state $|e\rangle$, the dit in state $|\uparrow\rangle$ pushes the wit to the ground state, hence, on average an equal amount of energy is extracted from or deposited into the classical field. In the case where we were to use only one wit–dit pair with the dit in state $|\downarrow\rangle$, only half of the energy gained in the working cycle would originate from the thermal bath, while the other half would have to be provided by the classical field. As the thermally excited wits on average contain less than $\Delta_{\rm w}$ on energy, the difference W_- to the final energy $\Delta_{\rm w}$ after the p̃SWAP operation has to be provided by the classical field, see Eq. (26).

The $\hat{u}_{1/4}$ operations changing the wit's energies in the p̃SWAP can be realized by letting the wits coherently exchange energy with a classical field in resonance with their energy spacing $\Delta_{\rm w}$. Assuming a dipolar interaction of the wits (featuring a dipole matrix element d) with a coherent field of strength E_0, see Ref. [42], this operation can be described by the Hamiltonian $\hat{H}_{\rm dip} = -E_0\left(d\,|e\rangle\langle g| + d^*\,|g\rangle\langle e|\,\right)\cos(\Delta_{\rm w}t)$. Within a rotating-wave approximation, the field-driven evolution of the working qubits involves Rabi-oscillations with a frequency $\Omega = E_0|d|/2$. Keeping the wit during the time $\tau_{1/4} = \pi/4\Omega$ in resonance with the field, the corresponding unitary transformation of the basis states $\{|e\rangle, |g\rangle\}$ is given by Eq. (13) with the phase $\varphi = \arg(d)$.

The above feature introduces a distinct difference between the pSWAP operations used in the sections II and III above and the p̃SWAP used in the operation of the quantum thermodynamic engine discussed here. While the logical operation, a partial swap, is common to both versions, the second implementation additionally features an energetic context. This energy context is required in order to transform thermal energy into work and impacts on the operation of this p̃SWAP. In particular, the logical operation can only be executed when the implementation respects the conservation of physical quantities, here, the conservation of energy. Furthermore, this conservation of energy has to be achieved with a classical energy reservoir in order to avoid entanglement between the wits and the reservoir. In fact, such an entanglement would reduce the possible energy gain from the wit and generate an additional waste heat, a feature we want to avoid with our implementation.

Two further remarks are in place at this point: i) No energy has been transferred from the working cycle to the demon qubits. This is different from the setups discussed in Refs. [10] and [12], where part of the heat absorbed in the wits is wasted by its transfer to the non-degenerate dits (with energy separation $\Delta_{\rm d}$), leading to a reduction in efficiency $\eta = 1 - \Delta_{\rm d}/\Delta_{\rm w}$ at best. The setup in Ref. [35] makes use of energy-degenerate systems both for the wits and dits and consumes purity of the dits in order to extract work from a single reservoir. Although, the latter setup is optimal (i.e., it extracts the maximum possible work for a given purity), it involves a slow adiabatic process. Specifically, in this machine, the heat is extracted in an isothermal process during which the wit adiabatically absorbs energy from the reservoir (i.e., this step involves a slow increase of $\Delta_{\rm w}$). In contrast, our engine operates at a constant $\Delta_{\rm w}$, i.e., the isothermal process is replaced by an isochoric process in our cycle. The advantage of the latter is that it does not require adiabatic heating, such that the cycle time is restricted only by the time of the p̃SWAP operation, assuming a fast equilibration time T_1 between the wit and the thermal reservoir. Provided that the two CNOT operations can be done much faster than the Rabi-period, the whole process of work extraction then requires only half a Rabi-period of time. ii) The above energy balance ignores the energy needed to purify the demon qubits for use in a next cycle. The entropy δS that has been transferred to the dits can be dealt with in a separate entropy cycle. This is justified by the fact that no energy is transferred between the wits and dits, hence the engine operates with mutually isolated energy- and entropy cycles. This additional step then accounts for the Second Law of Thermodynamics (and Landauer's principle) which thus is fully respected by the combined energy and entropy cycles.

In order to take the demon qubits back into the pure operational states $|\uparrow\rangle$ and $|\downarrow\rangle$, one may bring them into thermal contact with a second reservoir at a temperature $T_{\rm d}$ and adiabatically disbalance their levels in order to establish a new pure state. The energetic cost of disbalancing and rebalancing the levels is given by the Helmholtz free energy $\delta F_{\rm d} = -T_{\rm d}\delta S$ of the process. With $\delta S = S(\hat{r}_+) + S(\hat{r}_-) - S(\hat{r}_\uparrow) - S(\hat{r}_\downarrow) = 2\ln Z + Q/T$, we have to invest an amount $W_{\rm in} = 2T_{\rm d}\ln Z + (T_{\rm d}/T)\,Q$ of work to restore the dit's purities. We then arrive at a maximal overall efficiency

$$\eta_{2-{\rm cy}} = \frac{W_{\rm out} - W_{\rm in}}{Q} = 1 - \frac{T_{\rm d}}{T} - \frac{T_{\rm d}}{\Delta_{\rm w}}\frac{\ln Z}{p_e}, \qquad (27)$$

below the value $\eta_{\rm C} = 1 - T_{\rm d}/T$ of the Carnot cycle, even for the idealized machine. The net work $W_{\rm out} - W_{\rm in} =$

$Q - T_{\rm d}\delta S < Q$ produced by the engine is positive if $\beta_{\rm d}\Delta_{\rm w} > \beta\Delta_{\rm w} + (1+e^{\beta\Delta_{\rm w}})\ln(1+e^{-\beta\Delta_w})$. Hence, a positive work-yield requires that the temperature $T_{\rm d}$ of the demon reservoir is lower than T. In fact, for a hot working reservoir $\beta\Delta_{\rm w} \ll 1$, the minimal temperature of the cold reservoir is defined by the energy-level spacing $\Delta_{\rm w}$, $\beta_{\rm d}\Delta_{\rm w} > (2+\beta\Delta_{\rm w})\ln 2$ and only weakly depends on T. The opposite regime with $\beta\Delta_{\rm w} \gg 1$ requires that $\beta_{\rm d}\Delta_{\rm w} > \beta\Delta_{\rm w} + 1$.

The operational separation into distinct energy and entropy cycles with no energy transfer in between is the most interesting feature of this quantum-thermodynamic engine. It implies that all the heat Q absorbed from the thermal reservoir by the working qubits in the energy cycle can be extracted after the demon's action, $W_{\rm out} = Q$, and hence the energy cylce locally runs with unit efficiency and does not produce any waste heat (under ideal operation). All work reduction $W_{\rm in}$ enforced by the Second Law is deferred to the entropy cycle which can be run in a separate location or even at another time, e.g., by preparing a reservoir of demon qubits which then can be 'consumed' later in the operation of the engine.

In the above protocol, we have assumed that the two demon qubits are prepared in perfectly pure states. If instead one allows a finite chaotic component in $\hat{r}^\epsilon_\uparrow = \epsilon\mathbb{1} + (1-2\epsilon)|\uparrow\rangle\langle\uparrow|$ and $\hat{r}^\epsilon_\downarrow = \epsilon\mathbb{1} + (1-2\epsilon)|\downarrow\rangle\langle\downarrow|$, then the resulting states of the wits take over this mixing after the p̃SWAP operation, $\hat{\rho}^\epsilon_g = \epsilon\mathbb{1} + (1-2\epsilon)|g\rangle\langle g|$ and $\hat{\rho}^\epsilon_e = \epsilon\mathbb{1} + (1-2\epsilon)|e\rangle\langle e|$. As a result, the possible gain in work is reduced: when extracting the energy from the second wit with the help of a half-period Rabi pulse $\hat{u}_{1/2}$, one may excite rather than de-excite the wit, $\hat{u}_{1/2}|g\rangle = ie^{i\varphi}|e\rangle$, a process that occurs with probability ϵ. The average extracted work thus is reduced to $W^\epsilon_+ = (1-\epsilon)\Delta_{\rm w} - \epsilon\Delta_{\rm w} = (1-2\epsilon)\Delta_{\rm w}$ and the total work gain is given by $W^\epsilon_{\rm out} = 2\Delta_{\rm w}(p_e - \epsilon)$. On the other hand, both wits remain excited with probability ϵ and hence the heat absorbed in the subsequent cycle is reduced correspondingly, $Q^\epsilon = 2\Delta_{\rm w}(p_e-\epsilon)$, leading again to a maximal engine efficiency $\eta^\epsilon = W^\epsilon_{\rm out}/Q^\epsilon = 1$. Nevertheless, one can extract work out of the heat bath only when the dits are initially more pure than the wits, i.e., for $\epsilon < p_e$.

When extending the discussion to include the entropy cycle, we have to determine the work required to bring the dits back to their original mixed states $\hat{r}^\epsilon_\uparrow$ and $\hat{r}^\epsilon_\downarrow$. The p̃SWAP operation in Eq. (23) results in mixed dit states of the form $\hat{r}^\epsilon_\pm = (1-\epsilon)\hat{r}_\pm + \epsilon\hat{r}_\mp$. In order to restore the dits to their original states, one needs to invest the external work $W^\epsilon_{\rm in} = T_{\rm d}\delta S^\epsilon$, with $\delta S^\epsilon = S(\hat{r}^\epsilon_+) + S(\hat{r}^\epsilon_-) - S(\hat{r}^\epsilon_\uparrow) - S(\hat{r}^\epsilon_\downarrow)$. Then, the net produced work $W^\epsilon_{2-{\rm cy}} = W^\epsilon_{\rm out} - W^\epsilon_{\rm in}$ is given by

$$W^\epsilon_{2-{\rm cy}} = 2\Delta_{\rm w}\left[p_e - \epsilon - \frac{H[p_e+\epsilon(1-2p_e)] - H[\epsilon]}{\Delta_{\rm w}\beta_{\rm d}}\right], \quad (28)$$

where $H[x] = -x\ln x - (1-x)\ln(1-x)$ denotes the Shanon entropy. Interestingly, $W^\epsilon_{\rm out}$ and $W^\epsilon_{\rm in}$ exhibit different functional dependencies on the dit impurity ϵ. E.g., for $p_e \to 1/2$ (hot regime) the work $W^\epsilon_{\rm in}$ required for only partial purification of the dit decreases more rapidly than the gain in $W^\epsilon_{\rm out}$. Hence, one can find an optimal value $\epsilon_{\rm w}$ which maximizes the work (28) generated per cycle or, in other words, the engine power. On the other hand, instead of maximizing the engine's power one can consider its efficiency by comparing the net work $W^\epsilon_{2-{\rm cy}}$ with the absorbed heat $Q^\epsilon = 2\Delta_{\rm w}(p_e-\epsilon)$,

$$\eta^\epsilon_{2-{\rm cy}} = 1 - \frac{H[p_e+\epsilon(1-2p_e)] - H[\epsilon]}{\beta_{\rm d}\Delta_{\rm w}(p_e-\epsilon)}, \quad (29)$$

and find the optimal dit impurity ϵ_η maximizing the engine's efficiency. In the following, we discuss the result of such an optimization and the emerging maximal power and efficiency of the optimized machine.

The complete dependence of the optimal values $\epsilon_{\rm w}$ and ϵ_η maximizing the power and efficiency of the engine on the parameters p_e and $\beta_{\rm d}\Delta_{\rm w}$ has to be found numerically (see appendix) and the result is shown in Fig. (7). For a hot working reservoir with $\beta\Delta_w \ll 1$ and $p_e \to 1/2$ one can find the approximate expressions

$$\epsilon_{\rm w} \approx \left\{1 + \exp\left[\beta_{\rm d}\Delta_{\rm w} + H'[p_e](1-2p_e)\right]\right\}^{-1}, \quad (30)$$

$$\epsilon_\eta \approx p_e - \frac{1}{2}(1-2p_e) + \frac{2}{3}(1-2p_e)^3, \quad (31)$$

where $H'[x] = \ln[(1-x)/x]$ is the derivative of $H[x]$. Note that ϵ_η depends only on β (via p_e), while $\epsilon_{\rm w}$ involves both temperatures β and $\beta_{\rm d}$. Quite surprisingly, in the hot regime with $p_e \to 1/2$, the optimal efficiency is reached at ϵ-values close to $1/2$, see also Eq. (31), i.e., for almost chaotic demon qubits. However, at the same time the absorbed heat Q^ϵ goes to zero and so does the work $W^\epsilon_{2-{\rm cy}}$, i.e., we deal with an optimal engine but one that generates no power, see Fig. 8. Indeed, the optimal power is attained at lower values $\epsilon_{\rm w} < 1/2$ and this value decreases further when the demon reservoir's temperature $T_{\rm d}$ is lowered.

The corresponding efficiencies $\eta_{2-{\rm cy}}$ and powers $W^\epsilon_{2-{\rm cy}}$ for optimal dit impurities $\epsilon = \epsilon_{\rm w}$ and $\epsilon = \epsilon_\eta$ are shown in Fig. (8) as a function of the inverse heating temperature β and for a demon reservoir with $\beta_{\rm d}\Delta_{\rm w} = 2.0$. Also shown are the performances for an engine operating with pure dit states $\epsilon = 0$, which is always underperforming with respect to the efficiency. Moreover, for a hot demon reservoir with $\beta_{\rm d}\Delta_{\rm w} \leq 2\ln(2) \approx 1.39$, the ideal engine with $\epsilon = 0$ cannot produce positive work. On the other hand, the optimal engines with either $\epsilon = \epsilon_\eta$ or $\epsilon = \epsilon_{\rm w}$ can yield positive work for any temperature of the demon reservoir, though the operating regime $\beta \in [0, \beta_{\rm d}/2]$ is small at high temperatures $\beta_{\rm d}\Delta_{\rm w} \to 0$, see appendix. In the opposite situation of a cold demon reservoir $\beta_{\rm d}\Delta_{\rm w} \gg 1$ the temperature of the working reservoir is bound by $\beta\Delta_{\rm w} < \beta_{\rm d}\Delta_{\rm w} - 1$. The three efficiency curves $\eta^\epsilon_{2-{\rm cy}}(\beta)$ for $\epsilon = 0$, ϵ_η, $\epsilon_{\rm w}$ then approach one another near the critical value $\beta\Delta_{\rm w} \approx \beta_{\rm d}\Delta_{\rm w} - 1$. Finally, as is obvious from Fig. (8), the ϵ_η and $\epsilon_{\rm w}$ optimized engines never

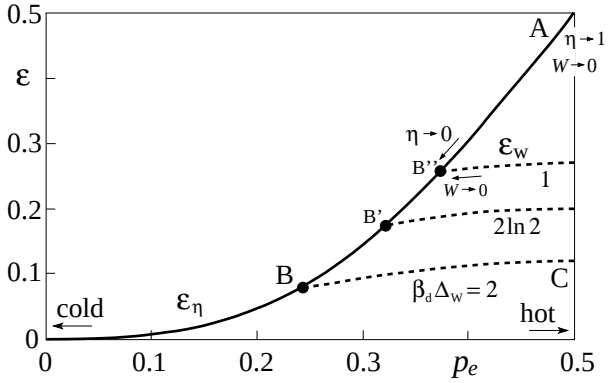

FIG. 7: Optimal values ϵ_η (solid line) and $\epsilon_{\rm W}$ (dashed lines) for the dit impurity ϵ versus occupation p_e of excited states. The three dashed lines correspond to different values $\beta_{\rm d}\Delta_{\rm w} = 1.0$ (upper curve), $\beta_{\rm d}\Delta_{\rm w} = 2\ln 2$ below which the ideal engine with $\epsilon = 0$ cannot produce positive work, and $\beta_{\rm d}\Delta_{\rm w} = 2$ (bottom curve). At point A, the efficiency $\eta^{\epsilon}_{2-{\rm cy}}$ approaches unity but the generated work $W^{\epsilon}_{2-{\rm cy}}$ goes to zero. At the points point B, B' and B" both $\eta^{\epsilon}_{2-{\rm cy}}$ and $W^{\epsilon}_{2-{\rm cy}}$ approach zero at fixed values of $\beta_{\rm d}\Delta_{\rm w}$ along the lines $\epsilon_\eta(p_e)$ and $\epsilon_{\rm W}(p_e, \beta_{\rm d})$ (note that ϵ_η does not depend on $\beta_{\rm d}$ and η approaches zero at different points along $\epsilon_\eta(p_e)$ for different values of $\beta_{\rm d}\Delta_{\rm w}$). At point C, the work per cycle reaches a value $W^{\epsilon}_{2-{\rm cy}} \approx 0.43\,\Delta_{\rm w}$ with an efficiency $\eta^{\epsilon}_{2-{\rm cy}} = 0.57$. The points A, B, and C reappear in Figure 8 below.

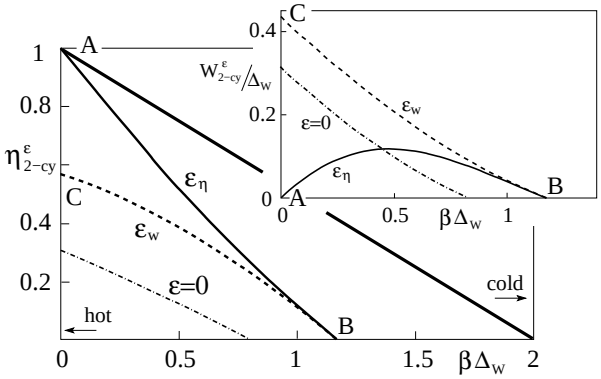

FIG. 8: Engine efficiencies $\eta^{\epsilon}_{2-{\rm cy}}$ and work per cycle $W^{\epsilon}_{2-{\rm cy}}$ (inset) at a fixed demon temperature $\beta_{\rm d}\Delta_{\rm w} = 2$ as a function of the dimensionless working temperature $\beta\Delta_{\rm w}$. Shown are the performances for the idealized machine with $\epsilon = 0$ (dash-dotted line; this line decreases with decreasing $\beta_{\rm d}\Delta_{\rm w}$ and disappears from the plot at $\beta_{\rm d}\Delta_{\rm w} \leq 2\ln(2) \approx 1.39$) and the efficiency- and power-optimized machines at $\epsilon = \epsilon_\eta$ (solid line) and $\epsilon = \epsilon_{\rm W}$ (dashed line). The thick solid upper line describes the Carnot efficiency $\eta_{\rm C} = 1 - T_{\rm d}/T$. Maximal efficiency but vanishing power is attained in A. On approaching B, both efficiency and power vanish. In C the power-optimized machine is characterized by both finite efficiency and power.

attain the Carnot efficiency, except for a very hot working reservoir, where

$$\eta^{\epsilon}_{2-{\rm cy}}(\beta \to 0, \beta_{\rm d}) \approx 1 - 2\frac{T_{\rm d}}{T}\Big(1 - \frac{(\beta\Delta_{\rm w})^2}{6}\Big), \qquad (32)$$

at $\epsilon = \epsilon_\eta$. In order to reach the Carnot efficiency, one has to use working qubits with a tunable level spacing and replace our isochoric heating by an adiabatic isothermal process as in Ref. [35].

VI. SUMMARY AND CONCLUSION

Quantum mechanics allows for processes that are classically forbidden. This idea can be pursued in the context of thermodynamics and the Second Law. In this work, we have investigated the possibility for an energy-isolated system to undergo an evolution with a decreasing entropy. In order to render this task non-trivial, one has to replace the classical concept of an 'isolated system' with an energy-isolated but open quantum system that can entangle with its (micro-)environment. This implies allowing a phase-exchange with the environment. Furthermore, the environment and its interaction with the system has to be properly engineered—rather than an uncontrolled macroscopic environment inducing incoherence, we had to consider a properly designed micro-environment.

With these prerequisites in mind and starting from the quantum-information-theoretic insight that unital quantum channels produce an evolution with non-decreasing entropy, we have searched for an energy-conserving non-unital quantum channel to reach our goal. Furthermore, we have considered a minimal two-qubit mesoscopic setting with a scattering electron (a flying system-qubit) that interacts with a micro-environment in the form of a spin (the demon qubit), interacting with the electron's current via its magnetic field. This approach naturally has led us to a process where the electron–spin (or system–demon) interaction generates two non-commuting rotations of the spin. An alternative setup with the spin replaced by a double-dot qubit allows for two equal interaction events but requires a qubit rotation in between, ultimately producing two non-commuting operations on the double-dot as well.

The analysis of these specific mesoscopic examples in terms of a quantum circuit has revealed a general scheme or algorithm that exerts a partial SWAP operation between the system and demon qubits. Swapping the system state against a purer or less mixed environmental state naturally explains the system's reduction in entropy or increase in coherence, where the latter is more easily observed in a direct interference experiment. Starting and ending with product states, the pSWAP process, although generating an intermediate strongly entangled system–environment state, ultimately does not entangle the system with its environment. While the system state can be chosen arbitrary, i.e., a pure superposition state or

any mixed state, the micro-environment has to be properly prepared, implying the provision of information to the system. Furthermore, within our scheme, the requirement of no net energy exchange between the system and the micro-environment is guaranteed by using an environmental qubit with energy-degenerate states. Note that the conservation of the subsystem's individual energies is a subtle issue as the partition of the interaction energy is not clear. We thus have used either a phase interaction, where this question does not appear at all, or have focused on the energy conservation between initial and final states.

The insight that the system's entropy decrease is based on a SWAP of states makes sure that nothing mysterious happens with the Second Law of thermodynamics, as the overall entropy of the system plus micro-environment is conserved. Rather, the micro-environment assumes the role of a quantum Maxwell demon and in this terminology the honoring of the Second Law corresponds to Landauer's principle applied in the restauration of the demon qubits. Comparing our quantum demon to Maxwell's original classical demon one notes that the latter as well reduces the system's entropy without taking up energy, i.e., the entropy flows without associated heat flow. The crucial difference between the classical and quantum demons is that the former makes use of information while the latter only uses purity. In particular, the information stored in the classical demon has to be read in order to operate the machine, as the next stroke depends on the measurement outcome. On the contrary, the information about the wit swapped to the quantum demon is never read and the engine can be operated in an autonomous manner.

A number of designs for quantum thermodynamic engines have been proposed, including such that make use of SWAP operations. Having focused on energy-isolated systems, our approach naturally has lead us to a design where the working (or system) cycle is energy-separated from the demon cycle. This feature provides the possibility to feed a heat engine with one local thermal reservoir, while providing purity from a distant source that can be handled independently. Such a design is useful when the thermal- to directed-energy conversion should be free from (uncontrolled) waste heat. As an alternative, one might trade the entropy in the thermally excited state against entropy stored in other, e.g., orbital[11], degrees of freedom of the same system. Analyzing the practical aspects of our design, we have found that the best machine is not the ideal one involving pure demon qubits, but that some degree of incoherence is favorable, both in terms of efficiency and power. The ideal machine with a vanishing demon impurity ϵ is recovered when optimizing the engine for maximal work at small demon temperatures $T_{\rm d}$.

Over many decades, Maxwell's demon has been a fascinating concept, despite his imprisonment by Landauer's principle. Our quantum Maxwell demon based on degenerate demon qubits and allowing for an energy-isolated operation of the working cycle is possibly as close as one could imagine to Maxwell's original idea of a demon.

Acknowledgments

We thank Renato Renner for discussions and acknowledge financial support from the National Science Foundation through the National Center of Competence in Research on Quantum Science and Technology (QSIT), the Pauli Center for Theoretical Studies at ETH Zurich, and the Russian Foundation for Basic Research under Grant No. 14-02-01287.

Appendix A: Quantum engine optimization

The optimal ϵ-values for the demon qubits which maximize either the engine work or power ($\epsilon = \epsilon_{\rm w}$) or engine efficiency ($\epsilon = \epsilon_\eta$) can be found by differentiating the corresponding target quantities ($W^\epsilon_{2-{\rm cy}}$ or $\eta^\epsilon_{2-{\rm cy}}$) with respect to ϵ, see Eqs. (28) and (29), with the relations

$$(1-2p_e)H'[p_e+\epsilon(1-2p_e)]-H'[\epsilon]=-\beta_{\rm d} \qquad \text{(A1)}$$

providing $\epsilon_{\rm w}$ and

$$\begin{aligned}\big[(1-2p_e)H'[p_e+\epsilon(1-2p_e)]-H'[\epsilon]\big](p_e-\epsilon)\\ +H[p_e+\epsilon(1-2p_e)]-H[\epsilon]=0\end{aligned} \qquad \text{(A2)}$$

the value for ϵ_η. These equations can be solved in the high-temperature regime $\beta\Delta_{\rm w}\gg 1$ where $p_e\to 1/2$ and which is governed by the small parameter

$$\xi = 1-2p_e = \frac{1-e^{-\beta\Delta_{\rm w}}}{1+e^{-\beta\Delta_{\rm w}}}. \qquad \text{(A3)}$$

Assuming $H'[p_e+\epsilon(1-2p_e)]=H'[p_e+\epsilon\xi]\approx H'[p_e]$ in (A1), one straightforwardly arrives at the result for $\epsilon_{\rm w}$ as given by Eq. (30).

Next, we find ϵ_η from Eq. (A2) using the ansatz $\epsilon_\eta = p_e-\delta p=(1-\xi)/2-\delta p$ with $\delta p>0$,

$$\begin{aligned}&\delta p\Big[\xi H'\big[(1-\xi^2)/2-\xi\delta p\big]-H'\big[(1-\xi)/2-\delta p\big]\Big]\\ &+H\big[(1-\xi^2)/2-\xi\delta p\big]-H\big[(1-\xi)/2-\delta p\big]=0.\end{aligned} \qquad \text{(A4)}$$

Expanding $H[x]$ and $H'[x]$ near $x=1/2$ (where $H'[1/2]=0$) up to the fourth and third order, respectively, one arrives at the algebraic equation

$$48(\delta p)^4+64\xi(\delta p)^3+24(\delta p)^2-6\xi^2+5\xi^4=0, \qquad \text{(A5)}$$

with the solution $\delta p\approx\xi/2-2\xi^3/3+O(\xi^5)$ producing the result Eq. (31).

Finally, we find the minimal temperature $T_{\rm m}$ (or maximal $\beta_{\rm m}$) where the engine provides positive work. For a fixed demon parameter $\beta_{\rm d}\Delta_{\rm w}$, the corresponding constraint on p_e and ϵ has the form (see Eq. (28)),

$$H[p_e+\epsilon(1-2p_e)]-H[\epsilon]=\beta_{\rm d}\Delta_{\rm w}(p_e-\epsilon). \qquad \text{(A6)}$$

For a power-optimized engine, $\epsilon = \epsilon_{\rm w}$, and combining (A6) with (A1) one immediately arrives at Eq. (A2). This implies that near $\beta_{\rm m}$ both curves $\epsilon_{\rm w}$ and ϵ_η coincide, resulting in the same engine efficiencies near the critical temperature. This observation explains the merging curves in Fig. (8) near $\beta_{\rm m}$. In the high-temperature regime $\beta_{\rm d}\Delta_{\rm w}, \beta\Delta_{\rm w} \ll 1$ one can substitute ϵ_η as given by Eq. (31) into (A6); an expansion with respect to $\xi \ll 1$ provides the approximate solution $\beta_{\rm m} \approx \beta_{\rm d}/2$.

[1] Sir W. Thomson, Mathematical and Physical Papers (Cambridge University Press, Cambridge, England, 1882).
[2] S. Carnot, Réflexions sur la puissance motrice de feuet sur les machines propres à dévelopder cette puissance (Bachelier, Paris, 1824).
[3] H. Spohn and J. Lebowitz, Advances in Chemical Physics: For Ilya Prigogine **38**, 109 (1978).
[4] R. Alicki, J. Phys. A **12**, L103 (1979).
[5] M. Horodecki, J. Oppenheim, Nat. Commun. **4**, 2059 (2013).
[6] F. Brandao, M. Horodecki, N. Ng, J. Oppenheim, and S. Wehner, PNAS **112**, 3275 (2015).
[7] P. Skrzypczyk, A.J. Short, and S. Popescu, Nat. Commun. **5**, 1 (2014).
[8] N. Linden, S. Popescu, and P. Skrzypczyk, Phys. Rev. Lett. **105**, 130401 (2010).
[9] N. Brunner, N. Linden, S. Popescu, and P. Skrzypczyk Phys. Rev. E **85**, 051117 (2012).
[10] S. Lloyd, Phys. Rev. A **56**, 3374 (1997).
[11] M.O. Scully, Phys. Rev. Lett. **87**, 220601 (2001).
[12] H.T. Quan, Y.D. Wang, Yu-xi Liu, C.P. Sun, and F. Nori, Phys. Rev. Lett. **97**, 180402 (2006).
[13] H.T. Quan, Yu-xi Liu, C.P. Sun, and F. Nori, Phys. Rev. E **76**, 031105 (2007).
[14] D. Venturelli, R. Fazio, and V. Giovannetti, Phys. Rev. Lett. **110**, 256801 (2013).
[15] P. Strasberg, G. Schaller, T. Brandes, and C. Jarzynski, Phys. Rev. E **90**, 062107 (2014).
[16] J.C. Maxwell, *Theory of Heat* (Appleton, London, 1871).
[17] L. Szillard, Z. Phys. **53**, 840 (1929).
[18] R. Landauer, IBM J. Res. Develop. **5**, 183 (1961).
[19] C.H. Bennett, Int. J. Theor. Phys. **21**, 905 (1982).
[20] C.H. Bennett, Studies in History and Philosophy of Modern Physics **34**, 501 (2003).
[21] H.-P. Breuer and F. Petruccione, *The Theory of Open Quantum Systems* (Oxford University Press, Oxford, 2002).
[22] S. Deffner and C. Jarzynski, Phys. Rev. X **3**, 041003 (2013).
[23] J.M. Horowitz and M. Esposito, Phys. Rev. X **4**, 031015 (2014).
[24] Note that the relative entropy $S(\hat\rho \parallel \hat\sigma) = {\rm Tr}[\hat\rho \ln \hat\rho - \hat\rho \ln \hat\sigma]$ is related to the entropy production rate, while here we are interested in the entropy itself.
[25] G. Lindblad, Comm. Math. Phys. **40**, 147 (1975).
[26] A.S. Holevo and V. Giovannetti, Rep. Prog. Phys. **75** 046001 (2012).
[27] G.B. Lesovik, A.V. Lebedev, I.A. Sadovskyy, M.V. Suslov, and V.M. Vinokur, Scientific Reports **6**, 32815 (2016).
[28] G. Mahler, Quantum Thermodynamic Processes: Energy and Information Flow at the Nanoscale (Taylor and Francis, Boca Raton, 2015)
[29] H.E.D. Scovil and E.O. Schulz-DuBois, Phys. Rev. Lett. **2**, 262 (1959).
[30] J.P. Palao, R. Kosloff, J.M. Gordon, Phys. Rev. E **64**, 056130 (2001).
[31] T. Feldmann and R. Kosloff, Phys. Rev. E **61**, 4774 (2000) and *ibid* **68**, 016101 (2003).
[32] D. Segal and A. Nitzan, Phys. Rev. E **73**, 026109 (2006).
[33] J.P. Pekola, D.S. Golubev, and D.V. Averin, Phys. Rev. B **93**, 024501 (2016).
[34] F. Tonner and G. Mahler, Phys. Rev. E **72**, 066118(2005).
[35] J.M. Diaz de la Cruz and M.A. Martin-Delgado, Phys. Rev. **A 89**, 032327 (2014).
[36] P.O. Boykin, T. Mor, V. Roychowdhury, F. Vatan, and R. Vrijen, Proc. Natl. Acad. Sci. **99**, 3388 (2002).
[37] J.M. Fernandez, S. Lloyd, T. Mor, and V. Roychowdhury, Int. J. of Quantum Inform. **2**, 461 (2004).
[38] G. Brassard, Y. Elias, T. Mor, and Y. Weinstein, Eur. Phys. J. Plus **129**, 258 (2014).
[39] N. Schuch and J. Siewert, Phys. Rev. A **67**, 032301 (2003).
[40] I. Procaccia and R. D. Levine, J. Chem. Phys. **65**, 3357 (1076).
[41] J. Åberg, Phys. Rev. Lett. **113**, 150402 (2014).
[42] L. Mandel and E. Wolf, Optical coherence and quantum optics (Cambridge University Press, Cambridge, 1995).
[43] F. Caruso, V. Giovannetti, C. Lupo, and S. Mancini, Rev. Mod. Phys. **86**, 1203 (2014).